

# Articles

## Creating Aligned Arrays of *Bacillus Megaterium* in Sol–Gel Matrixes

Shantang Liu,<sup>†</sup> Lynn F. Wood,<sup>‡</sup> Dennis E. Ohman,<sup>‡</sup> and Maryanne M. Collinson<sup>\*,†</sup>

Department of Chemistry, Virginia Commonwealth University, Richmond, Virginia 23284, and Department of Microbiology and Immunology, Virginia Commonwealth University, Richmond, Virginia 23298-0678

Received September 13, 2006. Revised Manuscript Received February 19, 2007

This paper describes a simple and convenient method for constructing an array of aligned bacteria and its immobilization in a solid framework. Paramagnetic particles were attached to *Bacillus megaterium* via the carbodiimide coupling between the amine functional groups on the particle with carboxylic acid groups on the bacteria. It was found that the amount of particles on the surface of the bacteria was dependent on the experimental conditions such as reaction time. After the surface of the bacteria was fully coated with the magnetic particles, the bacteria responded to an external magnetic force. By taking advantage of this property, two-dimensional arrays of bacteria were easily formed on a glass substrate over a large area both in aqueous solution and in a silica-based sol. The aligned wire-like structures were frozen in place via gelation of the sol. These structures are highly stable and reproducible and can be used to create nanostructured arrays on surfaces for the fabrication of novel chemical sensors or catalytic supports.

### Introduction

During the past decade, many studies on materials that exhibit unique hierarchically organized pore-solid architecture have been carried out due to their importance in the design of catalytic supports, sensors, and microfluidic devices.<sup>1–3</sup> The sol–gel process provides a promising approach to fabricate porous materials since the polymerization of appropriate organic or inorganic precursors is carried out under ambient conditions.<sup>4</sup> With use of different templates such as molecules, surfactants, single cells, and latex or glass spheres, the primary pore structure in sol–gel-derived materials can be organized in a three-dimensional network.<sup>5,6</sup>

Recent work has been focused on the use of living systems as templates to create unique two- and three-dimensional structures.<sup>7–10</sup> For example, Zink, Dunn, and co-workers have reported that ordered structures in the silica sol–gel films

can be generated by using living cells as a template.<sup>11</sup> Belcher and co-workers have used yeast and viruses to create unique nanostructures including nanoparticle arrays,<sup>12</sup> nanowires,<sup>13</sup> and nanorings.<sup>14</sup> Mann and co-workers have utilized bacteria threads to create zeolite fibers.<sup>15</sup> Pollen grains have also been used as templates.<sup>16</sup> Applications of organized nanostructures in solid-state electrochemical devices have already been shown.<sup>8,17</sup>

In this work, a very different approach has been taken that involves the alignment and subsequent immobilization of bacteria in a two-dimensional network. The method chosen involves attaching magnetic particles to the surface of bacteria and aligning the “magnetic bacteria” under a magnetic field. There are many examples where magnetic

\* To whom correspondence should be addressed.

<sup>†</sup> Department of Chemistry.

<sup>‡</sup> Department of Microbiology and Immunology.

- (1) Collinson, M. M. *Structure, Chemistry, and Applications of Sol-Gel Derived Materials*; Academic Press: San Diego, CA, 2001; Vol. 5: Chalcogenides Glasses and Sol-gel Materials.
- (2) Avnir, D.; Coradin, T.; Lev, O.; Livage, J. J. *Mater. Chem.* **2006**, *16*, 1013–1030.
- (3) Whitesides, G. M. *Nature* **2006**, *442*, 368–373.
- (4) Brinker, J.; Scherer, G. *Sol-Gel Science: The Physics and Chemistry of Sol-Gel Processing*; Academic Press: New York, 1990.
- (5) van Bommel, K. J. C.; Friggeri, A.; Shinkai, S. *Angew. Chem., Int. Ed.* **2003**, *42*, 980–999.
- (6) Kanungo, M.; Deepa, P. N.; Collinson, M. M. *Chem. Mater.* **2004**, *16*, 5535–5541.
- (7) Mann, S.; Burkett, S.; Davis, S. A.; Fowler, C. E.; Mendelson, N. H.; Sims, S. D.; Walsh, D.; Whilton, N. T. *Chem. Mater.* **1997**, *9*, 2300–2310.

- (8) Nam, K. T.; Kim, D. W.; Yoo, P. J.; Chiang, C. Y.; Meethong, N.; Hammond, P. T.; Chiang, Y. M.; Belcher, A. M. *Science* **2006**, *312*, 885–888.
- (9) Shenton, W.; Douglas, T.; Young, M.; Stubbs, G.; Mann, S. *Adv. Mater.* **1999**, *11*, 253.
- (10) Fujikawa, S.; Kunitake, T. *Langmuir* **2003**, *19*, 6545–6552.
- (11) Chia, S.; Urano, J.; Tamanoi, F.; Dunn, B.; Zink, J. I. *J. Am. Chem. Soc.* **2000**, *122*, 6488–6489.
- (12) Huang, Y.; Chiang, C. Y.; Lee, S. K.; Gao, Y.; Hu, E. L.; De Yoreo, J.; Belcher, A. M. *Nano Lett.* **2005**, *5*, 1429–1434.
- (13) Mao, C. B.; Solis, D. J.; Reiss, B. D.; Kottmann, S. T.; Sweeney, R. Y.; Hayhurst, A.; Georgiou, G.; Iverson, B.; Belcher, A. M. *Science* **2004**, *303*, 213–217.
- (14) Nam, K. T.; Peelle, B. R.; Lee, S. W.; Belcher, A. M. *Nano Lett.* **2004**, *4*, 23–27.
- (15) Zhang, B. J.; Davis, S. A.; Mendelson, N. H.; Mann, S. *Chem. Commun.* **2000**, 781–782.
- (16) Hall, S. R.; Bolger, H.; Mann, S. *Chem. Commun.* **2003**, 2784–2785.
- (17) Long, J. W.; Dunn, B.; Rolison, D. R.; White, H. S. *Chem. Rev.* **2004**, *104*, 4463–4492.

nanoparticles have been attached to biomolecules,<sup>18–23</sup> but very few that discuss their subsequent alignment. Examples of aligned nanostructures include those prepared from carbon nanotubes or microtubules where the magnetic nanoparticles were either attached to their surface or incorporated in them.<sup>24–27</sup>

This work focuses on the attachment of paramagnetic particles to *Bacillus megaterium*. *B. megaterium* was chosen as the “model” bacteria as it is a relatively large gram-positive rod-shaped bacteria ( $\sim 2 \times 10 \mu\text{m}$ ) that is easy to grow, is relatively harmless, and can form chains under flow.<sup>28</sup> When paramagnetic particles are first covalently attached to its surface via standard carbodiimide coupling,<sup>29</sup> it can be oriented under an external magnetic field to form long filaments in aqueous solution or in a silica-based sol. These filaments are tens to hundreds of micrometers in length and can be permanently locked in place upon gelation of the sol, leading to the possibility of creating ordered structures that can be etched to create channels for use in chemical and biochemical analysis or in microfluidic devices.

## Experimental Section

1-Ethyl-3-(3-dimethylaminopropyl)-carbodiimide hydrochloride (EDC), tetramethoxysilane (TMOS), methyltrimethoxysilane (MTMOS), and *N*-hydroxysuccinimide (NHS) were purchased from Aldrich-Sigma Chemical Co. BioMagPlus paramagnetic particles (iron oxide core with a silane coating, particle size  $< 1 \mu\text{m}$ ) containing surface amine groups were purchased from Polysciences, Inc. (Warrington, PA) and used as received. Glass cover slips were purchased from Ted Pella, Inc. (Redding, CA) and cleaned by successive sonication in acetone, ethanol, and water. Prior to use, they were plasma-cleaned (Harrick Plasma Cleaner) on high for 2 min. This treatment made the glass surface fully hydrophilic. Ultrapure water was obtained from a Millipore water purification system.

The bacteria were grown via standard protocols. Briefly, bacterial strains were grown in Luria broth (LB) at 37 °C with vigorous shaking for 18 h. Cells were harvested by centrifugation and washed with an equal volume of saline, and final cell pellets were resuspended in 15 mL of 0.85% NaCl solution (concentration of

bacteria was ca. 71.3 mg/mL). One milliliter of the suspended cells was centrifuged at 4000 rpm for 4 min.

To attach the paramagnetic particles to the bacteria, standard carbodiimide coupling was employed.<sup>29,30</sup> Approximately 50 mg of the wet bacteria was placed into 1 mL of 0.1 M phosphate buffer solution, pH = 7.2. Approximately 4–6 mg of EDC and 8 mg NHS were then added to the solution and the reaction was allowed to proceed for 30 min at room temperature with gentle shaking. The activated bacteria were separated by placing the suspension in a centrifuge tube and centrifuging at 4000 rpm for 3 min. The supernatant was then removed and the activated bacteria were resuspended in 1 mL of 0.1 M buffer solution. This washing procedure was repeated for at least three cycles to fully remove the excess EDC, EDC byproducts, and NHS. Finally, the bacteria were resuspended in 1 mL of 0.1 M buffer; 400  $\mu\text{L}$  (about 20 mg) of the magnetic particles was added and the reaction allowed to proceed for 3–24 h at room temperature with gentle shaking. An aliquot of resultant solution was pipetted onto a clean glass slide. Prior to AFM measurements, the sample was dried in a desiccator overnight. The alignment of the “magnetic bacteria” was done by placing a drop of solution on the glass substrate under an external magnetic field. All the optical images and videos were captured on a Sony CCD camera with WinTV Go-Plus for the digital recordings (Hauppauge Computer Inc., NY). The AFM images were acquired in the tapping mode on a Nanoscope III A multimode atomic force microscope (Digital Instruments, Veeco Metrology Group, Santa Barbara, CA) using ultrasharp silicon probes (MicroMasch) with spring constants of 20–70 N/m.

Sol A was prepared mixing 0.9 mL of H<sub>2</sub>O, 0.1 mL of TMOS, 0.1 mL of MTMOS, and 0.1 mL of 0.01 M HCl in a glass vial, while the sol solution B was prepared from 0.9 mL of H<sub>2</sub>O, 0.2 mL of TMOS, and 0.01 mL of 0.1 M HCl. A 100  $\mu\text{L}$  aliquot of the coated *B. megaterium* solution was added to 100  $\mu\text{L}$  of sol, and the resulting sol was vortexed for 10 s and then pipetted onto the glass surface.

## Results and Discussion

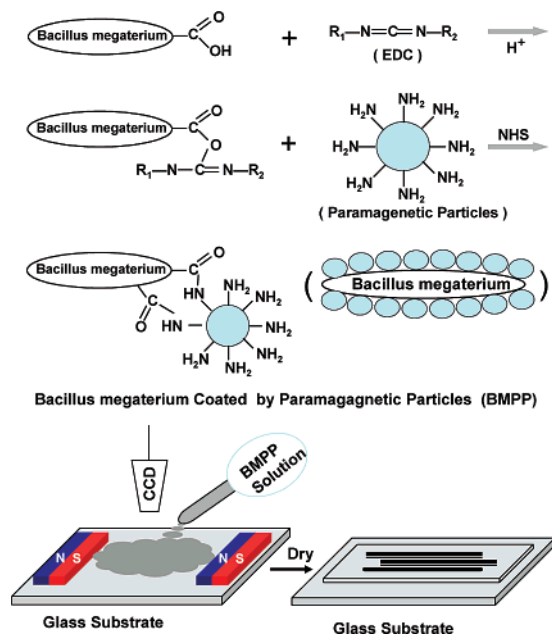
Figure 1 outlines the overall fabrication procedure. The procedure starts with the activation of carboxylic acid groups on the surface of *Bacillus megaterium* with EDC, followed by mixing it with the paramagnetic particles capped with the amino-terminated groups. By varying the reaction time, it was possible to obtain bacteria covered with a different number of magnetic particles.

Figure 2 shows the images and corresponding cross sections of the bacteria with and without the paramagnetic particles attached to its surface. The AFM measured heights of an individual activated bacterium (Figure 2A) and the activated bacteria after mixing with the paramagnetic particles for different reaction times (Figure 2B,C) are 535 nm, 1.09  $\mu\text{m}$ , and 1.17  $\mu\text{m}$ , respectively. The ca. 0.4–0.8  $\mu\text{m}$  height difference is a reasonable value of the addition of paramagnetic particles onto the bacteria surface.<sup>31</sup> A comparative analysis of the bacterium in the AFM image in Figure 2B reveals some particles are attached on only part of the surface. The observed height of the upper part of the

- (18) Dreyfus, R.; Baudry, J.; Roper, M. L.; Fermigier, M.; Stone, H. A.; Bibette, J. *Nature* **2005**, *437*, 862–865.
- (19) Rossi, L. M.; Quach, A. D.; Rosenzweig, Z. *Anal. Bioanal. Chem.* **2004**, *380*, 606–613.
- (20) Dyal, A.; Loos, K.; Noto, M.; Chang, S. W.; Spagnoli, C.; Shafi, K.; Ulman, A.; Cowman, M.; Gross, R. A. *J. Am. Chem. Soc.* **2003**, *125*, 1684–1685.
- (21) Koh, I.; Wang, X.; Varughese, B.; Isaacs, L.; Ehrman, S. H.; English, D. S. *J. Phys. Chem. B* **2006**, *110*, 1553–1558.
- (22) Ho, K. C.; Tsai, P. J.; Lin, Y. S.; Chen, Y. C. *Anal. Chem.* **2004**, *76*, 7162–7168.
- (23) Gu, H. W.; Ho, P. L.; Tsang, K. W. T.; Wang, L.; Xu, B. *J. Am. Chem. Soc.* **2003**, *125*, 15702–15703.
- (24) Platt, M.; Muthukrishnan, G.; Hancock, W. O.; Williams, M. E. *J. Am. Chem. Soc.* **2005**, *127*, 15686–15687.
- (25) Hutchins, B. M.; Hancock, W. O.; Williams, M. E. *Phys. Chem. Chem. Phys.* **2006**, *8*, 3507–3509.
- (26) Correa-Duarte, M. A.; Grzelczak, M.; Salgueirino-Maceira, V.; Giersig, M.; Liz-Marzan, L. M.; Farle, M.; Sieradzki, K.; Diaz, R. *J. Phys. Chem. B* **2005**, *109*, 19060–19063.
- (27) Cao, A. Y.; Zhang, X. F.; Wei, J. Q.; Li, Y. H.; Xu, C. L.; Liang, J.; Wu, D. H.; Wei, B. Q. *J. Phys. Chem. B* **2001**, *105*, 11937–11940.
- (28) Katz, E.; Yarin, A. L.; Salalha, W.; Zussman, E. *J. Appl. Phys.* **2006**, *100*, 034313-1.
- (29) Collinson, M. M.; Bowden, E. F.; Tarlov, M. J. *Langmuir* **1992**, *8*, 1247–1250.

(30) Details for the procedure for EDC/NHS cross-linking of carboxylates with primary amines on the paramagnetic particles can refer to EDC product instructions from [www.piercenet.com](http://www.piercenet.com).

(31) The AFM measured height of the paramagnetic particles on the glass fall within the range 90–750 nm with the average size of  $360 \pm 50$  nm.



**Figure 1.** Schematic representation of the attachment of paramagnetic colloidal particles to *B. megaterium* and its alignment under an external magnetic field. Not drawn to scale.

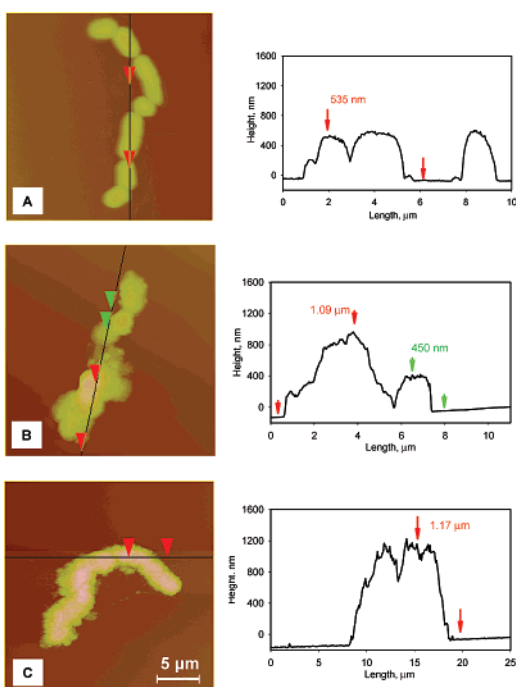


**Figure 2.** AFM topographic images and corresponding distance–height profiles of activated *B. megaterium* (A) and activated *B. megaterium* after mixing with paramagnetic particles for 6 (B) and 24 h (C). The Z-scale for the AFM images is 2500 nm.

bacterium is in the range 450–600 nm, which is in good agreement with the height of unmodified bacteria (Figure 2A). The lower part has a height of 1.1  $\mu\text{m}$ , consistent with particles on its surface. This result indicates that only part of the surface of *Bacillus megaterium* is affixed with particles. After a longer reaction time, a higher local particle density on most of the bacteria is apparent (Figure 2C). In all cases with a reaction time greater than 16 h, the particles faithfully cover the whole surface, thus confirming the validity of the attachment strategy outlined in Figure 1.

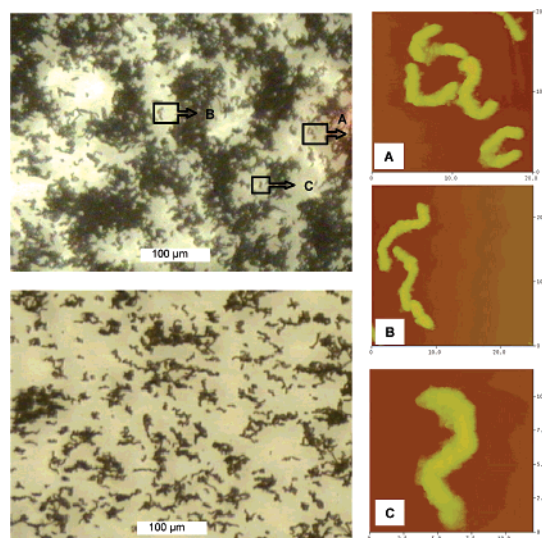


**Figure 3.** Optical and AFM images of *B. megaterium* coated with paramagnetic colloidal particles in the absence of an external field on a glass substrate. The left-bottom optical image is the coated *B. megaterium* in buffer solution and the left-upper is after drying. The right column of AFM topographic images are those of the individual bacterium marked by squares in the upper optical image. The Z-scale for the AFM images is 2500 nm.

Previous researchers have shown that magnetic particles can be attached to carbon nanotubes<sup>26,27</sup> and microtubules<sup>24,25</sup> or form filaments or wires<sup>32–36</sup> that can be aligned in a magnetic field. We employed a similar method to align modified *B. megaterium* under an external magnetic field. Figure 3 shows optical images of an ensemble of modified *B. megaterium* in the absence of external magnetic field. The lower optical image shows the “magnetic bacteria” in water; the upper is after the water has evaporated. The bacteria in the dried sample form randomly scattered or aggregate structures with multilayering. From the AFM images of a few bacteria in the dried sample, it can be clearly seen that the modified bacteria still form the hair-like structure, indicating there is no preferred orientation even though the surface is covered with magnetic particles. If the unmodified bacteria (those without EDC treatment) are mixed with the paramagnetic particles, AFM images show isolated bacteria in the presence of isolated particles (see Figure 1S in Supporting Information).

The alignment of modified *B. megaterium* with the magnetic field lines of an external magnet was visualized by recording optical micrographs of them in two different solutions on glass. Figure 4 shows images of the bacteria under an external magnetic field with different directions. The modified *B. megaterium* forms long chains along the magnetic lines and the chains move when the magnet is moved to remain oriented in the direction of the field. When the magnetic field directions changes from Figure 4A to 4B

- (32) Goubault, C.; Jop, P.; Fermigier, M.; Baudry, J.; Bertrand, E.; Bibette, J. *Phys. Rev. Lett.* **2003**, *91*, 2608002-1.
- (33) Goubault, C.; Leal-Calderon, F.; Voivy, J.; Bibette, J. *Langmuir* **2005**, *21*, 3725–3729.
- (34) Sheparovych, R.; Sahoo, Y.; Motornov, M.; Wang, S.; Luo, H.; Prasad, P. N.; Sokolov, I.; Minko, S. *Chem. Mater.* **2006**, *18*, 591–593.
- (35) Furst, E. M.; Suzuki, C.; Fermigier, M.; Gast, A. P. *Langmuir* **1998**, *14*, 7334–7336.
- (36) Vuppu, A. K.; Garcia, A. A.; Hayes, M. A. *Langmuir* **2003**, *19*, 8646–8653.



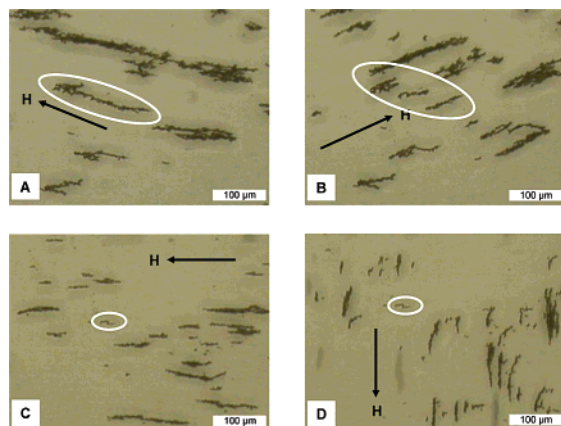


**Figure 4.** Optical micrographs of coated *B. megaterium* aligned in buffer on a glass substrate in the presence of an external field with field directions as indicated. Realignment took place by moving the magnetic field from (A) to (B) and from (C) to (D).

and Figure 4C to 4D, the aligned chains begin to move with the magnetic field and some “wires” break into several short chains as indicated by the large white circles. Occasionally, some bacteria do not move with the magnetic field direction as shown in the small white circles in images C and D of Figure 4. This is likely caused either by the strong interaction between the *B. megaterium* and the glass substrate or by these particular bacteria possibly having fewer magnetic particles attached to their surfaces and thus being less responsive in the presence of an external field. No alignment or movement can be observed for *B. megaterium* without the attached magnetic particles in a magnetic field. Optical micrographs look similar to those shown in Figure 3. The aligned filaments are also not just aligned particles as most of the particles are small ( $<1\ \mu\text{m}$ ) and thus difficult to see in an optical micrograph without being attached to something much larger, i.e., *B. megaterium*.

These results clearly demonstrate that magnetic *B. megaterium* can be manipulated in an external field and can be used as building blocks to fabricate the hierarchical two-dimensional chain structures. To permanently fix these chain structures and thus use them as a template for further device fabrication, we exploited the sol–gel process using two kinds of sols. The advantage of the sol–gel process is that the sol is very fluid and entities that are doped into it can move as easily as they do in water. As soon as the sol turns into a gel, the movement of large entities stops and their orientation is permanently fixed. Leventis, Rolison, and co-workers have elegantly shown this with aligned magnetic particles in an aerogel.<sup>37</sup> Previous work has also shown that these entities (i.e., templates) can be removed from this framework to create “replicas” with the same three-dimensional structure.<sup>10</sup>

The sol (sol A or sol B) containing modified *B. megaterium* was placed on the glass slide. Figure 5 shows *B. megaterium* aligned parallel to the magnetic field in the silica-based sol. As the sol starts to cross-link, its viscosity increases and at some point it becomes a gel (the TMOS only sol gels faster than the one with MTMOS).

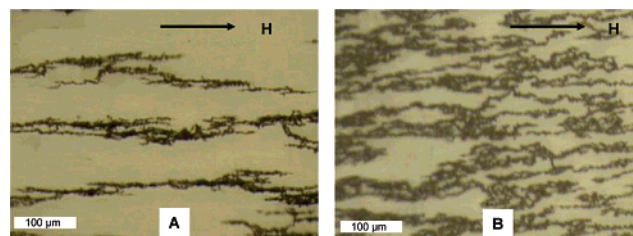


**Figure 5.** Optical images of aligned wire structures of modified *B. megaterium* in Sol A (left) and Sol B (right) in the presence of an external field in the direction indicated.

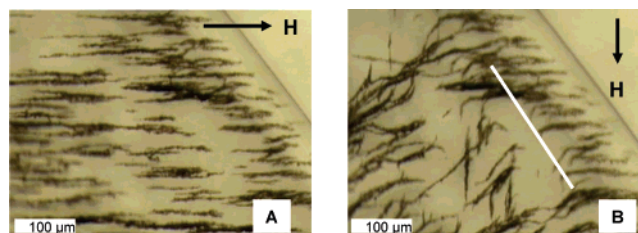


**Figure 6.** Aligned “filaments” of modified *B. megaterium* in Sol A during the sol-to-gel transition in the presence of an external field (left image) and after the magnetic field was rotated  $90^\circ$  (right image). The area to the right of the white line is the gel and the area to the left is the sol.

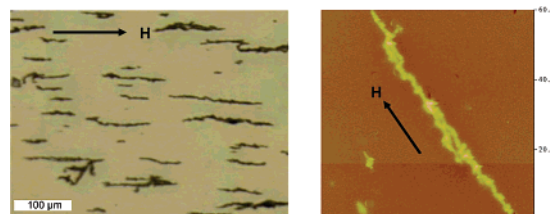


**Figure 7.** Optical image (left) and AFM topographic image (right) of aligned wire-like structures of modified *B. megaterium* in the gel formed from Sol A. The magnetic bacteria were aligned in the sol in the presence of an external field in the direction indicated. After gelation, the external field was removed and the images were acquired. The Z-scale for the  $60 \times 60\ \mu\text{m}$  AFM image is 1000 nm.

In Figure 6, the transition between the sol state (marked by fluidity) and the gel state (marked by macroscopic rigidity) can be observed. In this experiment, a drop of the bacteria-doped sol was placed on a clean glass slide and a magnetic field was applied to align the bacteria in the direction of the magnetic field lines (Figure 6A). At some point in time, the sol started to gel from the outside to the inside. At this point, the magnetic field was moved  $90^\circ$  degrees. The bacteria residing in the sol (fluid) reoriented while those in the gel (rigid) did not (Figure 6B). The gelling line (sol–gel transition) is marked in the figure.

Figure 7 shows aligned filaments of *B. megaterium* encapsulated in the gel after the magnetic field was removed. Once the filaments are formed and aligned in the sol and the sol gelled, the magnetic field can be removed (or its direction changed) and the bacteria do not move. From the AFM images, it is clearly observed that coated *B. megaterium* encapsulated in the gel are stretched along the magnetic field direction to form thin “wire-like” structures. These bacterial threads are fixed in the orientation imposed on them by the external magnetic field while they were in the sol.

## Conclusions

In summary, using *B. megaterium* and a very simple and straightforward experimental procedure, we have succeeded

(37) Leventis, N.; Elder, I. A.; Long, G. J.; Rolison, D. R. *Nano Lett.* **2002**, *2*, 63–67.

in creating aligned arrays of bacteria both in aqueous solution and in a silica sol. The advantage of using a sol is that these aligned bacterial filaments can be frozen in place and in a specific orientation determined by an external magnet when the sol turns into a gel. In a simplistic analogy, *B. megaterium* modified with the magnetic particles can be thought of as a synthetic mimic of magnetotactic bacteria in that they both contain iron oxide particles.<sup>38,39</sup> In magnetotactic bacteria, the magnetic particles are located in the intracellular organelles whereas in the synthetic version it is on the outside. Both respond to an external magnetic field. An example of another synthetic mimic is the swollen bacterial-magnetite threads prepared by Mann and co-workers.<sup>40,41</sup> In that study, a bacterial thread prepared from *B. subtilis* was swollen and subsequently doped with 10 nm iron nanoparticles when placed in ferrofluid. The magnetic particles in this case lie

between the cell walls. The present study has a number of intriguing advantages that these others studies do not easily offer including the ability to (1) extend it to other bacteria, particularly those of a different size and shape, (2) remove the bacteria to create arrays of long hollow capsules or cavities in films for drug delivery or supports for chemical sensors, and (3) create interesting architectures and patterns by employing surfaces with magnetic patterns.<sup>42</sup> Future work will proceed in this direction.

**Acknowledgment.** We gratefully acknowledge support of this work by the National Science Foundation (CHE-0618220). A special thanks goes to Everett Carpenter for helpful suggestions regarding magnetic nanoparticles.

**Supporting Information Available:** Section analysis of AFM image. This material is available free of charge via the Internet at <http://pubs.acs.org>.

CM062188C

(38) Scheffel, A.; Gruska, M.; Faivre, D.; Linaroudis, A.; Graumann, P. L.; Plitzko, J. M.; Schuler, D. *Nature* **2006**, *441*, 248–248.

(39) Simmons, S. L.; Bazyliniski, D. A.; Edwards, K. J. *Science* **2006**, *311*, 371–374.

(40) Meldrum, F. C.; Heywood, B. R.; Mann, S. *Science* **1992**, *257*, 522–523.

(41) Wong, K. K. W.; Douglas, T.; Gider, S.; Awschalom, D. D.; Mann, S. *Chem. Mater.* **1998**, *10*, 279–285.

(42) Kimura, T.; Sato, Y.; Kimura, F.; Iwasaka, M.; Ueno, S. *Langmuir* **2005**, *21*, 830–832.